

Direct Uncertainty Quantification

Yadi Wei¹ Roni Khardon¹

Abstract

Traditional neural networks are simple to train but they produce overconfident predictions, while Bayesian neural networks provide good uncertainty quantification but optimizing them is time consuming. This paper introduces a new approach, direct uncertainty quantification (DirectUQ), that combines their advantages where the neural network directly models uncertainty in output space, and captures both aleatoric and epistemic uncertainty. DirectUQ can be derived as an alternative variational lower bound, and hence benefits from collapsed variational inference that provides improved regularizers. On the other hand, like non-probabilistic models, DirectUQ enjoys simple training and one can use Rademacher complexity to provide risk bounds for the model. Experiments show that DirectUQ and ensembles of DirectUQ provide a good tradeoff in terms of run time and uncertainty quantification, especially for out of distribution data.

1. Introduction

With the development of training and representation methods for deep learning, models using neural networks provide excellent predictions. However, such models fall behind in terms of uncertainty quantification and their predictions are often overconfident (Guo et al., 2017). Bayesian methods provide a methodology for uncertainty quantification by placing a prior over parameters and computing a posterior given observed data, but the computation required for such methods is often infeasible. Variational inference (VI) is one of the most popular approaches for approximating the Bayesian outcome, e.g., (Blundell et al., 2015; Graves, 2011; Wu et al., 2019). By minimizing the KL divergence between the variational distribution and the true posterior and constructing an evidence lower bound (ELBO), one can find the best approximation to the intractable posterior. How-

ever, when applied to deep learning, VI requires sampling to compute the ELBO, and it suffers from both high computational cost and large variance in gradient estimation. Wu et al. (2019) have proposed a deterministic variational inference (DVI) approach to alleviate the latter problem. The idea of this approach relies on the central limit theorem, which implies that with sufficiently many hidden neurons, the distribution of each layer forms a multivariate Gaussian distribution. Thus we only need to compute the mean and covariance of each layer. However, DVI still suffers from high computational cost and complex optimization.

Inspired by DVI, we observe that the only aspect that affects the prediction is the distribution of the last layer in the neural network. We therefore propose to use a neural network to directly output the mean and the diagonal covariance of the last layer, which avoids calculating a distribution over network weights and saves intermediate computations. Like all Bayesian methods, our method quantifies both epistemic and aleatoric uncertainty of the output. However, it does so in an explicit manner, so we call it *Direct Uncertainty Quantification* (DirectUQ). DirectUQ has a single set of parameters and thus enjoys simple optimization as in non-Bayesian methods yet it has the advantage of uncertainty quantification in predictions similar to Bayesian methods.

We can motivate DirectUQ from several theoretical perspectives. First, due to its simplicity, one can derive risk bounds for the model through Rademacher complexity. Second, DirectUQ can be derived as an alternative ELBO for neural networks which uses priors and posteriors on the output layer. We show that, for the linear case, with expressive priors DirectUQ can capture the same predictions as standard variational inference. With practical priors and deep networks the model can be seen as a simpler alternative. Third, through the interpretation as ELBO, we derive improved priors (or regularizers) for DirectUQ motivated by collapsed variational inference (Tomczak et al., 2021) and empirical bayes (Wu et al., 2019). The new regularizers greatly improve the performance of DirectUQ.

An experimental evaluation compares DirectUQ with VI and non-Bayesian neural networks optimized by stochastic gradient descent (SGD), as well as ensembles of these models. The results show that (1) DirectUQ is slightly slower than SGD but much faster than VI, and (2) Direc-

¹Luddy School of Informatics, Computing, and Engineering, Indiana University, Bloomington, Indiana, USA. Correspondence to: Roni Khardon <rkhardon@iu.edu>.

tUQ achieves better uncertainty quantification on shifted and out-of-distribution data while preserving the quality of in-distribution predictions. Overall, ensembles of DirectUQ provide good tradeoff in terms of run time and uncertainty quantification especially for out-of-distribution data.

1.1. Related Work

DirectUQ shares some similarities with [Kendall & Gal \(2017\)](#), where both use neural networks to output the mean and covariance of the last layer. However, unlike their method DirectUQ represents a variational lower bound, and there are differences in the loss function and approach for epistemic uncertainty which are elaborated further in Section 2. Another similar line of work ([Sun et al., 2019](#); [Tran et al., 2022](#)) performs variational inference on the functional space. However, they focus on choosing a better prior in weight space which is induced from Gaussian Process priors on functional space, whereas DirectUQ directly puts a simple prior in function space.

DirectUQ differs from existing variational inference methods. Last-layer variational inference ([Brosse et al., 2020](#)) performs variational inference on the weights of the last layer, while we perform variational inference on the output of the last layer. The local reparametrization trick ([Tomczak et al., 2020](#); [Oleksiienko et al., 2022](#)) performs two forward passes with the mean and variance to sample the output for each layer, while we only require one pass and sample the output of the last layer for prediction.

Various alternative Bayesian techniques have been proposed. One direction is to get samples from the true posterior, as in Markov chain Monte Carlo methods ([Wenzel et al., 2020](#); [Izmailov et al., 2021](#)). Expectation propagation aims to minimize the reverse KL divergence to the true posterior ([Teh et al., 2015](#); [Li et al., 2015](#)). These Bayesian methods, including variational inference, often suffer from high computational cost and therefore hybrid methods were proposed. Stochastic weight averaging Gaussian ([Maddox et al., 2019](#)) forms a Gaussian distribution over parameters from the stochastic gradient descent trajectory. Dropout ([Gal & Ghahramani, 2016](#)) randomly sets weights 0 to model the epistemic uncertainty. Deep ensembles ([Lakshminarayanan et al., 2017](#)) use ensembles of models learned with random initialization and shuffling of data points and then average the predictions. These methods implicitly perform approximate inference. In addition to these methods, there are also non-Bayesian methods to calibrate the overconfident predictions, for example, temperature scaling ([Guo et al., 2017](#)) introduces a temperature parameter to anneal the predictive distribution to avoid high confidence. DirectUQ strikes a balance between simplicity and modelling power to enable simple training and Bayesian uncertainty quantification.

2. Direct Uncertainty Quantification

In this section we describe our DirectUQ method in detail. Given a neural network parametrized by weights W and input x , the output layer is $z = f_W(x)$. In classification, z is a k -dimensional vector, where k is the number of classes. The probability of being class i is defined as

$$p(y = i|z) = \text{softmax}(z)_i = \frac{\exp z_i}{\sum_j \exp z_j}. \quad (1)$$

In regression, $z = (m, l)$ is a 2-dimensional vector. We apply a function g on l that maps l to a positive real number. The probability of the output y is:

$$p(y|z) = \mathcal{N}(y|m, l) = \frac{1}{\sqrt{2\pi g(l)}} \exp\left(-\frac{(y - m)^2}{2g(l)}\right). \quad (2)$$

Traditional non-Bayesian deep learning learns weights by minimizing $-\log p(y|z)$ using stochastic gradient descent. We refer to this as SGD.

By fixing the weights W , SGD maps x to z deterministically, while Bayesian methods seek to map x to a distribution over z . Variational inference puts a distribution over W and marginalizes out to get a distribution over z . According to central limit theorem, with sufficiently wide neural network, the marginalization distribution of z is normal ([Wu et al., 2019](#)). DirectUQ pursues this in a direct manner. It has two sets of weights, W_1 and W_2 (with shared components), to model the mean and variance of z . That is, $\mu_q(x) = f_{W_1}(x)$, $\sigma_q(x) = g(f_{W_2}(x))$, where $g : \mathbb{R} \rightarrow \mathbb{R}^+$ maps the output to positive real numbers as the variance is positive. Thus, $q(z|x) = \mathcal{N}(z|\mu_q(x), \text{diag}(\sigma_q^2(x)))$, where $\mu_q(x)$, $\sigma_q^2(x)$ are vectors of the corresponding dimension. We will call $q(z|x)$ the *variational predictive distribution*.

Note the the prediction over y is given by $\int q(z|x)p(y|z)dz$ which is different from the basic model. In regression, the basic model of Eq (2) is known as the mean-variance estimator ([Kabir et al., 2018](#); [Khosravi et al., 2011](#); [Kendall & Gal, 2017](#)). Applying DirectUQ on this model, we will have **four** outputs, two of which are the means of m and l , and the other two are the variances of m and l . The mean of l represents the heteroscedastic aleatoric uncertainty and the variances of m and l model the epistemic uncertainty as the variances come from marginalization of Bayesian posteriors. In classification, using Eq (1), the mean of z induces aleatoric uncertainty and the variance of z represents epistemic uncertainty.

The standard Bayesian approach puts a prior on the weights W . Instead, since DirectUQ models the distribution over z , we put a prior over z . We consider two options, a conditional prior $p(z|x)$ and a simpler prior $p(z)$. Both of these choices

yield a valid ELBO using the same steps:

$$\begin{aligned} \log p(y|x) &\geq \mathbb{E}_{q(z|x)} \left[\log \frac{p(y, z|x)}{q(z|x)} \right] \\ &= \mathbb{E}_{q(z|x)} [\log p(y|z)] - \text{KL}(q(z|x) || p(z|x)). \end{aligned} \quad (3)$$

Eq (3) is defined for every (x, y) . For a dataset $\mathcal{D} = \{(x, y)\}$, we optimize W_1 and W_2 such that:

$$\sum_{(x, y) \in \mathcal{D}} \left\{ \mathbb{E}_{q(z|x)} [\log p(y|z)] - \text{KL}(q(z|x) || p(z|x)) \right\}$$

is maximized. We regard the negation of the first term $\mathbb{E}_{q(z|x)} [-\log p(y|z)]$ as the loss term and treat $\text{KL}(q(z|x) || p(z|x))$ as a regularizer. In practice, we put a coefficient η on the regularizer, as is often done in variational approximations (Higgins et al., 2017). Then, from a regularized loss minimization view, our objective becomes:

$$\min_{W_1, W_2} \sum_{(x, y) \in \mathcal{D}} \left\{ \mathbb{E}_{q(z|x)} [-\log p(y|z)] + \eta \text{KL}(q(z|x) || p(z|x)) \right\}. \quad (4)$$

In most cases, the loss term is intractable, so we use Monte Carlo samples to approximate it, where implementations can use reparametrization to reduce the variance in gradients:

$$\mathbb{E}_{q(z|x)} [-\log p(y|z)] \approx \frac{1}{M} \sum_{m=1}^M -\log p(y|z^{(m)}), \quad (5)$$

where $z^{(m)} \sim q(z|x)$.

We can now discuss the relation to Kendall & Gal (2017) in more details. This work also draws samples in the output space but replaces the loss term in Eq (5) with the cross entropy loss, $-\log \frac{1}{M} \sum_m p(y|z^{(m)})$. Furthermore, they use dropout and their objective has no explicit regularization, whereas our formulation yields a valid ELBO.

3. Rademacher Complexity of DirectUQ

In this section we provide generalization bounds for DirectUQ through Rademacher Complexity. We need to make the following assumptions.

Assumption 3.1. $\log p(y|z)$ is L_0 -Lipschitz in z , i.e., $\log p(y|z) - \log p(y|z') \leq L_0 \|z - z'\|_2$.

Assumption 3.2. The link function g is L_1 -Lipschitz.

We show in the Appendix that these assumptions hold for classification and with a smoothed loss for regression. With the two assumptions, we derive the main result:

Theorem 3.3. *Let \mathcal{H} be the set of functions that can be represented with neural networks with parameter space \mathcal{W} , $\mathcal{H} = \{f_W(\cdot) | W \in \mathcal{W}\}$. DirectUQ has two components, so the DirectUQ hypothesis class is $\mathcal{H} \times \mathcal{H}$*

= $\{(f_{W_1}(\cdot), f_{W_2}(\cdot)) | W = (W_1, W_2), W_1, W_2 \in \mathcal{W}\}$. Let l be the loss function for DirectUQ, $l(W, (x, y)) = E_{q_W(z|x)} [-\log p(y|z)]$. Then the Rademacher complexity of DirectUQ is bounded as $R(l \circ (\mathcal{H} \times \mathcal{H}) \circ S) \leq (L_0(1 + L_1)K) \cdot R(\mathcal{H} \circ S)$, where K is the dimension of z .

Proof. We show that the loss is Lipschitz in $f_{W_1}(x)$ and $f_{W_2}(x)$. Fix any x , and W, W' . We denote the mean and standard deviation of $q_W(z|x)$ by μ and s and the same for $q_{W'}(z|x)$.

$$\begin{aligned} &\mathbb{E}_{q_W(z|x)} [-\log p(y|z)] - \mathbb{E}_{q_{W'}(z|x)} [-\log p(y|z)] \\ &= \mathbb{E}_{\epsilon \sim \mathcal{N}(0, I)} [\log p(y|\mu' + \epsilon \cdot s') - \log p(y|\mu + \epsilon \cdot s)] \\ &\leq \mathbb{E}_{\epsilon \sim \mathcal{N}(0, I)} [L_0 \|(\mu - \mu') + \epsilon \cdot (s - s')\|_2] \\ &\leq L_0 \|\mu - \mu'\|_2 + L_0 \mathbb{E}_\epsilon [\sqrt{\epsilon^2 (s - s')^2}] \\ &\leq L_0 \|\mu - \mu'\|_2 + L_0 \sqrt{\mathbb{E}_\epsilon [\epsilon^2 (s - s')^2]} \\ &= L_0 (\|\mu - \mu'\|_2 + \|s - s'\|_2) \\ &\leq L_0 (\|\mu - \mu'\|_1 + \|s - s'\|_1) \end{aligned}$$

where the third equation uses the Lipschitz assumption and the fifth uses Jensen's inequality. In the above equations the product and power are performed element-wise, and the derivation holds for multivariate z . The loss function is Lipschitz in μ , which is exactly $f_{W_1}(x)$. Further, s is L_1 -Lipschitz in the logit $f_{W_2}(x)$, thus, the loss function is $(L_0(1 + L_1))$ -Lipschitz in $f_{W_1}(x)$ and $f_{W_2}(x)$. The theorem follows from Rademacher complexity bounds for bivariate functions (Lemma A.1) and for functions over vectors (Corollary A.2). \square

Hence Rademacher complexity for DirectUQ is bounded through the Rademacher complexity of deterministic neural networks. This shows one advantage of DirectUQ which is more amenable to analysis than standard VI due to its simplicity. The Rademacher complexity for neural networks is $O\left(\frac{B_W B_x}{\sqrt{N}}\right)$ (Golowich et al., 2018), where B_W bounds the norm of the weights and B_x bounds the input. The Rademacher complexity of DirectUQ is of the same order.

4. Comparison of DirectUQ and VI

DirectUQ is inspired by deterministic variational inference and it highly reduces the computational cost. We explore whether DirectUQ can produce exactly the same predictive distribution as VI. In this section, we show that this is the case for linear models but that for deep models DirectUQ is less powerful. We first introduce the setting of linear models. Let the parameter be θ , then the model is defined as:

$$y|x, \theta \sim p(y|\theta^\top x). \quad (6)$$

For example, $p(y|\theta^\top x) = \mathcal{N}(y|\theta^\top x, \frac{1}{\beta})$ where β is a constant for Bayesian linear regression; and $p(y = 1|\theta^\top x) =$

$\frac{1}{1+\exp(-\theta^\top x)}$ for Bayesian binary classification.

The standard approach specifies the prior of θ to be $p(\theta) = \mathcal{N}(\theta|m_0, S_0)$, and uses $q(\theta) = \mathcal{N}(\theta|m, S)$. Then the ELBO objective for linear models with a dataset (X_N, Y_N) of size N , where $X_N = (x_1, x_2, \dots, x_N) \in \mathbb{R}^{d \times N}$ and $Y_N = (y_1, y_2, \dots, y_N) \in \mathbb{R}^N$, is:

$$\begin{aligned} & \sum_{i=1}^N \mathbb{E}_{q(\theta)} [\log p(y_i|\theta^\top x_i)] - \text{KL}(q(\theta)||p(\theta)) \\ &= \sum_{i=1}^N \mathbb{E}_{q(\theta)} [\log p(y_i|\theta^\top x_i)] - \frac{1}{2} [\text{tr}(S_0^{-1}S) - \log |S_0^{-1}S|] \\ & \quad - \frac{1}{2} (m - m_0)^\top S_0^{-1} (m - m_0). \end{aligned} \quad (7)$$

As the following theorem shows, if we use a conditional correlated prior and a variational posterior that correlates data points, then in the linear case DirectUQ can recover the ELBO and the solution of VI.

Theorem 4.1. *Let $p(z|X_N) = \mathcal{N}(z|m_0^\top X_N, X_N^\top S_0 X_N)$ be a correlated and data-specific prior (which means that for different data x , we have a different prior over z), and $q(z|x) = \mathcal{N}(z|\theta_1^\top x, x^\top V_2 x)$ be the variational predictive distribution of z , where θ_1 and V_2 are the parameters to be optimized. Then the DirectUQ objective is equivalent to the ELBO objective implying identical predictive distributions.*

Proof. The DirectUQ objective is:

$$\begin{aligned} & \sum_{i=1}^N \left\{ \mathbb{E}_{q(z|x_i)} [\log p(y_i|z)] \right\} - \text{KL}(q(z|X_N)||p(z|X_N)) \\ &= \sum_{i=1}^N \left\{ \mathbb{E}_{q(z|x_i)} [\log p(y_i|z)] \right\} \\ & \quad - \frac{1}{2} \text{tr}((X_N^\top S_0 X_N)^{-1} (X_N^\top V_2 X_N)) \\ & \quad + \frac{1}{2} \log |(X_N^\top S_0 X_N)^{-1} (X_N^\top V_2 X_N)| \\ & \quad - \frac{1}{2} (\theta_1^\top X_N - m_0^\top X_N)^\top (X_N^\top S_0 X_N)^{-1} (\theta_1^\top X_N - m_0^\top X_N). \end{aligned} \quad (8)$$

Assume $N > d$. First consider the loss term. Let L be the Cholesky decomposition of V_2 , i.e. $V_2 = LL^\top$. By reparametrization, for $\epsilon \sim \mathcal{N}(0, I_d)$, $\theta_1^\top x_i + x_i^\top L\epsilon \sim \mathcal{N}(\theta_1^\top x_i, x_i^\top LL^\top x_i)$ and thus

$$\begin{aligned} \mathbb{E}_{q(z|x_i)} [\log p(y_i|z)] &= \mathbb{E}_{\epsilon \sim \mathcal{N}(0, I_d)} [\log p(y_i|\theta_1^\top x_i + x_i^\top L\epsilon)] \\ &= \mathbb{E}_{\epsilon \sim \mathcal{N}(0, I_d)} [\log p(y_i|(\theta_1 + L\epsilon)^\top x_i)] \\ &= \mathbb{E}_{\theta \sim \mathcal{N}(\theta_1, LL^\top)} [\log p(y_i|\theta^\top x_i)], \end{aligned} \quad (9)$$

where the last equality uses reparametrization in a reverse order. By aligning $\theta_1 = m$ and $V_2 = LL^\top = S$, we

recognize that Eq (9) is exactly the loss term in Eq (7). Thus the low-dimensional posterior on z yields the same loss term as the high-dimensional posterior over W .

For the regularization, we use the pseudo inverse

$$(X_N^\top S_0 X_N)^{-1} = X_N^\top (X_N X_N^\top)^{-1} S_0^{-1} (X_N X_N^\top)^{-1} X_N$$

and the same for V_2 . Then the regularization term in Eq (7) can be simplified to:

$$\begin{aligned} & - \text{KL}(q(z|X_N)||p(z|X_N)) \\ &= -\frac{1}{2} \text{tr}(S_0^{-1}V_2) + \frac{1}{2} \log |S_0^{-1}V_2| \\ & \quad - \frac{1}{2} (\theta_1 - m_0)^\top S_0^{-1} (\theta_1 - m_0). \end{aligned} \quad (10)$$

By aligning $\theta_1 = m$, $V_2 = S$, we can see that eq (10) is exactly the same as the regularizer in eq (7). \square

However, as the next theorem shows, for the non-linear case even if we ignore the prior we may not be able to recover the loss term exactly.

Theorem 4.2. *Given a neural network f_W parametrized by W and a mean-field Gaussian distribution $q(W)$ over W , there may not exist a set of parameters \tilde{W} such that for all input x we have $\mathbb{E}_{q(W)} [f_W(x)] = f_{\tilde{W}}(x)$.*

Proof Sketch. Consider the neural network with only one hidden unit and only one input. No matter what \tilde{W} we choose, there exists some region of x such that $f_{\tilde{W}}(x) = 0$ due to the non-linear activation. However, $\mathbb{E}_{q(W)} [f_W(x)]$ will include two segments of non-zero functions due to the properties of truncated normal distribution, thus, there is no \tilde{W} that can perfectly recover $\mathbb{E}_{q(W)} [f_W(x)]$. \square

The results of this section point to the potential and limitations of DirectUQ in terms of expressiveness relative to standard VI. In practice, computing a correlated and data-specific prior $p(z|x)$ is complex, and tuning its hyperparameters would be challenging. Hence, for a practical algorithm we propose to use a simple prior $p(z)$ independent of x . In addition, to reduce computational complexity, we do not learn a full covariance matrix and focus on the diagonal approximation. This limits expressive power but enables fast training of ensembles of DirectUQ.

5. Collapsed VI Applied to DUQ

Bayesian methods are often sensitive to the choice of prior parameters. To overcome this, Wu et al. (2019) used empirical Bayes (EB) to select the value of the prior parameters, and Tomczak et al. (2021) proposed collapsed variational inference, which defined a hierarchical model and performed inference on the prior parameters as well. Empirical Bayes

can be regarded as a special case of collapsed variational inference. In this section, we show how this idea is applicable in DirectUQ. In addition to z , we model the prior mean μ_p and variance σ_p^2 as Bayesian parameters. Now the prior becomes $p(z|\mu_p, \sigma_p^2)p(\mu_p, \sigma_p^2)$ and the variational distribution is $q(z|x)q(\mu_p, \sigma_p^2)$. Then the objective becomes:

$$\begin{aligned} \log p(y|x) &\geq \mathbb{E}_{q(z|x)q(\mu_p, \sigma_p^2)} \left[\log \frac{p(y, z, \mu_p, \sigma_p^2|x)}{q(z|x)q(\mu_p, \sigma_p^2)} \right] \\ &= \mathbb{E}_{q(z|x)} [\log p(y|z)] - \mathbb{E}_{q(\mu_p, \sigma_p^2)} [\text{KL}(q(z|x)||p(z|\mu_p, \sigma_p^2))] \\ &\quad - \text{KL}(q(\mu_p, \sigma_p^2)||p(\mu_p, \sigma_p^2)). \end{aligned} \quad (11)$$

Similar to eq (4), we treat the first term as a loss term and the other two terms as a regularizer along with a coefficient η and aggregate over all data. Since the loss term does not contain μ_p and σ_p^2 , we can get the optimal $q^*(\mu_p, \sigma_p^2)$ by optimizing the regularizer and the choice of η will not affect $q^*(\mu_p, \sigma_p^2)$. Then we can plug in the value of q^* into Eq (11). We next show how to compute $q^*(\mu_p, \sigma_p^2)$ and the final collapsed variational inference objective. The derivations are similar to the ones in (Tomczak et al., 2021) but they are applied on z not on W . In the following, we use K to denote the dimension of z .

5.1. Learn mean, fix variance

Let $p(z|\mu_p) = \mathcal{N}(z|\mu_p, \gamma I)$, $p(\mu_p) = \mathcal{N}(\mu_p|0, \alpha I)$. Then $q^*(\mu_p|x)$ is

$$\arg \min_{q(\mu_p)} \mathbb{E}_{q(\mu_p)} [\text{KL}(q(z|x)||p(z|\mu_p))] + \text{KL}(q(\mu_p)||p(\mu_p)),$$

and the optimal $q^*(\mu_p|x)$ can be computed as:

$$\log q^*(\mu_p|x) \propto -\frac{(\mu_q(x) - \mu_p)^\top (\mu_q(x) - \mu_p)}{2\gamma} - \frac{\mu_p^\top \mu_p}{2\alpha},$$

and $q^*(\mu_p|x) = \mathcal{N}(\mu_p|\frac{\alpha}{\alpha+\gamma}\mu_q(x), \frac{\alpha\gamma}{\alpha+\gamma})$. Notice that unlike the prior $q^*(\mu_p)$ depends on x . If we put q^* back in the regularizer of eq (11), the regularizer becomes:

$$\begin{aligned} &\frac{1}{2\gamma} \left[1^\top \sigma_q^2(x) + \frac{\gamma}{\gamma + \alpha} \mu_q(x)^\top \mu_q(x) \right] - \frac{1}{2} 1^\top \log \sigma_q^2(x) \\ &+ \frac{K}{2} \log(\gamma + \alpha) - \frac{K}{2}. \end{aligned} \quad (12)$$

As in (Tomczak et al., 2021), one thing to observe from eq (12) is that it puts a factor $\frac{\gamma}{\gamma+\alpha} < 1$ in front of $\mu_q(x)^\top \mu_q(x)$, which weakens the regularization on $\mu_q(x)$. We refer to this method as “duq-mean”.

5.2. Learn both mean and variance

Let $p(z|\mu_p, \sigma_p^2) = \mathcal{N}(z|\mu_p, \sigma_p^2)$, $p(\mu_p) = \mathcal{N}(\mu_p|0, \frac{1}{t}\sigma_p^2)$, $p(\sigma_p^2) = \mathcal{IG}(\sigma_p^2|\alpha, \beta)$, where \mathcal{IG} indicates the inverse

Gamma distribution. The posterior of μ_p is Gaussian and the posterior of σ_p^2 is inverse Gamma. In this case we can show that $q^*(\mu_p|x) = \mathcal{N}(\mu_p|\frac{1}{t+1}\mu_q(x), \frac{1}{(1+t)}\sigma_p^2)$ and $q^*(\sigma_p^2|x) = \mathcal{IG}(\sigma_p^2|(\alpha + \frac{1}{2})1, \beta + \frac{t}{2(t+1)}\mu_q(x)^2 + \frac{1}{2}\sigma_q^2(x))$ and the regularizer becomes

$$(\alpha + \frac{1}{2})1^\top \log \left[\beta 1 + \frac{t}{2(1+t)}\mu_q(x)^2 + \frac{1}{2}\sigma_q^2(x) \right] \quad (13)$$

$$- \frac{1}{2} 1^\top \log \sigma_q^2(x). \quad (14)$$

We refer to this method as “duq-mv”.

5.3. Empirical Bayes

Let $p(\sigma_p^2) = \mathcal{IG}(\sigma_p^2|\alpha, \beta)$, $p(z|\sigma_p^2) = \mathcal{N}(z|0, \sigma_p^2)$ and let $q(\sigma_p^2)$ be a delta distribution $\delta(s^*(x))$. Then the regularizer of eq (11) becomes:

$$\text{KL}(q(z|x)||p(z|\sigma_p^2)) - \log p(\sigma_p^2). \quad (15)$$

By minimizing this objective we obtain the optimal value $s^*(x) = \frac{\mu_q(x)^\top \mu_q(x) + 1^\top \sigma_q^2(x) + 2\beta}{K + 2\alpha + 2}$. Plugging this value into the KL term we obtain:

$$\begin{aligned} &\frac{1}{2} \left[K \log \frac{\mu_q(x)^\top \mu_q(x) + 1^\top \sigma_q^2(x) + 2\beta}{K + 2\alpha + 2} - 1^\top \log |\sigma_q^2(x)| \right] \\ &- \frac{K}{2} + \frac{1}{2} \frac{(K + 2\alpha + 2)(\mu_q(x)^\top \mu_q(x) + 1^\top \sigma_q^2(x))}{\mu_q(x)^\top \mu_q(x) + 1^\top \sigma_q^2(x) + 2\beta}. \end{aligned} \quad (16)$$

Following (Wu et al., 2019), as shown in appendix B.3, including the prior term in the regularizer reduces its complexity and this harms performance in practice. Hence, we use Eq (16) as the regularizer. We call this method “duq-eb”.

5.4. L2 regularization

Notice that all regularizations above are regularizing the variational predictive distribution $q(z|x)$, not the parameters of the neural network. By analogy to MAP solutions of Bayesian neural networks, we can also regularize the weights directly by replacing the regularizers with $\frac{\eta}{N} \|W\|_2$ in the objective, even though our posterior is on z . We include this in our experiments and call it “duq-l2”.

6. Experiments

In this section, we compare the empirical performance of DirectUQ with VI and hybrid methods related to stochastic gradient descent, as well as dropout (Gal & Ghahramani, 2016). VI candidates include the VI algorithm (Blundell et al., 2015) with fixed prior parameters (called vi-naive below), and other variations from collapsed variational inference (Tomczak et al., 2021) and empirical Bayes (Wu et al.,

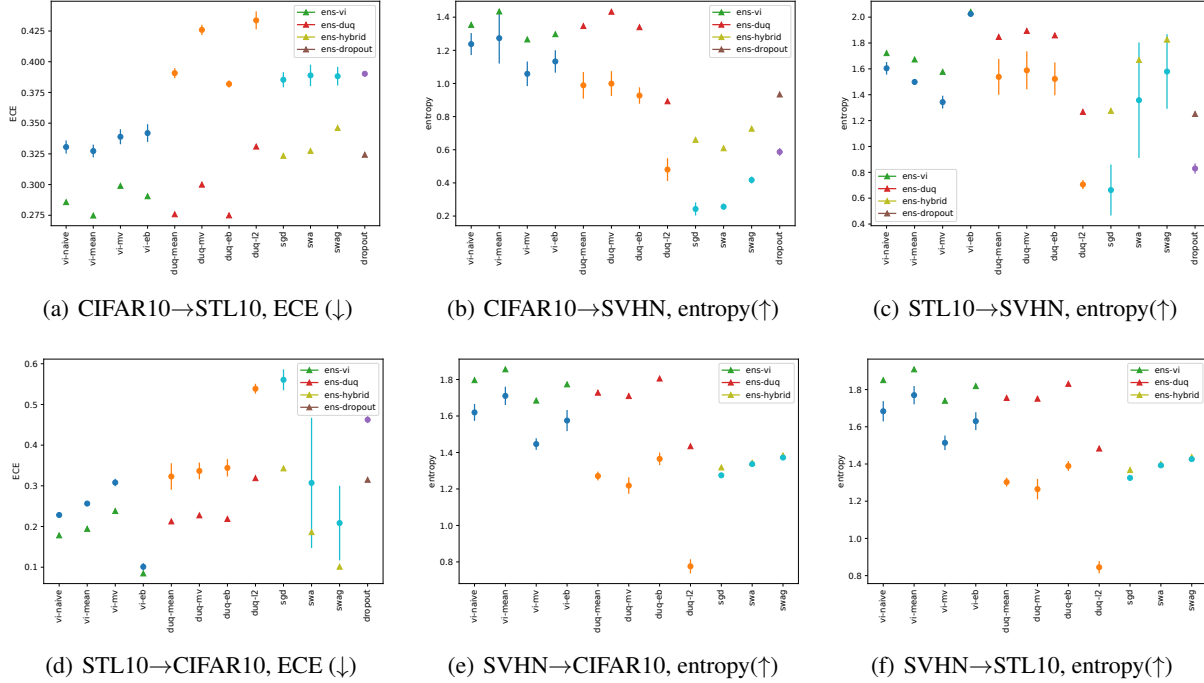


Figure 1: Uncertainty Quantification on AlexNet

2019). The hybrid methods include the non-Bayesian network optimized by stochastic gradient descent (marked as SGD below), as well as stochastic weight averaging (SWA, which uses the average of the SGD trajectory as the final weights) from Izmailov et al. (2018) and SWA-Gaussian (SWAG, which uses the SGD trajectory to form a Gaussian distribution over the neural network weight space) from Maddox et al. (2019). These methods are called hybrid methods because they do not have an explicit prior distribution over parameters but they can be interpreted as Bayesian methods. In addition to comparing the single-model performance of these methods, we compare their ensembles. The performance of each method is evaluated by the log loss on the test datasets and by two uncertainty quantification measures on shifted and out-of-distribution datasets.

6.1. Experiment Details

We examine our methods on small datasets using a fully connected single layer neural network and on large image datasets using more complex neural network structures. DirectUQ is implemented such that W_1 and W_2 share all weights except the last layer. For the first set of experiments, we pick four regression datasets and four classification datasets from the UCI repository (Dua & Graff, 2017), and use a single-layer neural network with 50 hidden units. We split every dataset into 80%/10%/10% for training, validation and testing and perform standard nor-

malization so that we do not need to tune hyperparameters for every dataset. For VI and DirectUQ, we select $\eta \in \{0.1, 0.3, 0.5, 0.7, 0.9, 1.0, 3.0, 5.0, 7.5, 10.0\}$ based on the validation log loss; for SGD, SWA and SWAG, we select weight decay in the same range as η . Since the neural network is small, we do not include dropout in comparison. For the second set of experiments, we use four image datasets, CIFAR10, CIFAR100, SVHN¹, STL10, together with two types of neural networks, AlexNet (Krizhevsky et al., 2012) and PreResNet20 (He et al., 2016), and fix $\eta = 0.1$ (except in “duq-l2” where we use $\eta = 5.0$) and the dropout rate 0.1. Note that using $\eta = 1$ in VI yields poor predictions (see Appendix) and using $\eta = 0.1$ provides a stronger baseline. In all experiments, we use the Adam optimizer for VI and DirectUQ. For hybrid methods, we adapt the code from previous work (Izmailov et al., 2018; Maddox et al., 2019) and use the stochastic gradient descent optimizer for SGD, SWA and SWAG. Ensemble models use 5 runs with different random initializations and batch orders. Other details such as hyperparameters, learning rate and number of epochs are given in the Appendix.

6.2. Run Time

Ignoring the data preprocessing time, we compare the run time of training 1 epoch of VI, DirectUQ and SGD. In Table

¹Dropout for SVHN on AlexNet fails and gives trivial uniform predictions, so we did not include it in the results.

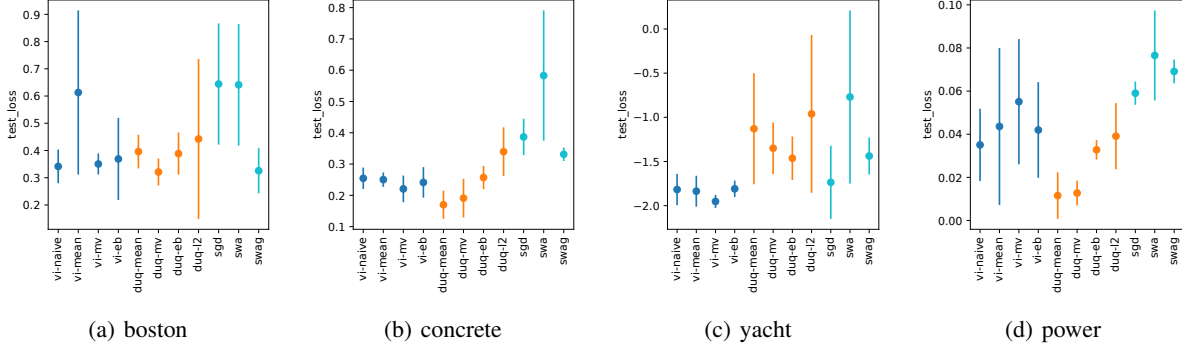


Figure 2: Test log loss on UCI regression datasets. Each dot with the error bar shows the mean and standard deviation of 5 independent runs. The standard deviations for some methods are very small.

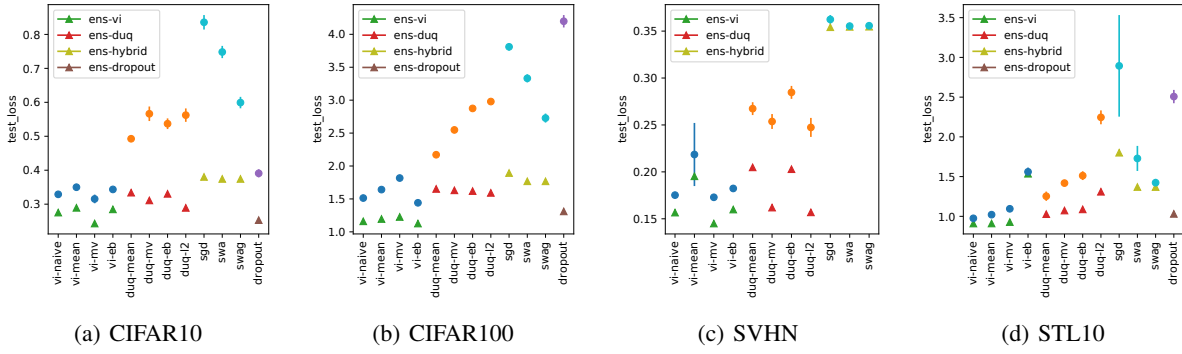


Figure 3: Test log loss of four image datasets on AlexNet. Each dot with error bar represents the mean and standard deviation of 5 independent runs and the triangle represents the ensemble of each method that aggregate these 5 runs for prediction (same for Figure 8). The standard deviations for some VI and DUQ methods are very small.

1 we show the mean and standard deviation of 10 runs of these methods. Different regularizers have a small effect in terms of run time, so we only show that of vi-naive for VI and duq-mean for DirectUQ. As shown in Table 1, DirectUQ is much faster than VI and is slightly slower than SGD.

This is as expected because if we set the sample size to be M , then SGD only needs 1 forward pass without sampling per batch, DirectUQ needs 1 forward pass and M samples of size K per batch, and VI needs M samples of the neural network size and M forward passes per batch. In addition, as the sample size M or the number of batches increases, the advantage of DirectUQ over VI expands as the increased forward passes will take more time, but the advantage of SGD over DirectUQ remains the same as sampling in a smaller space can be done in nearly constant time.

6.3. Uncertainty Quantification for Shifted and Out-of-distribution Data

In this section we examine whether DirectUQ can capture the uncertainty in predictions for shifted and out-of-

distribution (OOD) data. For uncertainty under data shift, STL10 and CIFAR10 can be treated as a shifted dataset for each other, as the figure size of STL10 is different from CIFAR10, and STL10 shares some classes with CIFAR10 so the labels are meaningful. Thus we can use expected calibration error (ECE, (Naeini et al., 2015)) to measure the uncertainty. That is, we separate data into bins of the same size according to the confidence level, calculate the difference between the accuracy and the averaged confidence in each bin and then average the differences among all bins, see Ovdia et al. (2019) for details. We select the number of bins to be 20. For uncertainty under OOD data, we choose the SVHN dataset as an OOD dataset for CIFAR10, as SVHN contains images of digits and the labels of SVHN are not meaningful in the context of CIFAR10. Thus, we cannot compute the accuracy. Instead, we use the entropy to measure the uncertainty. For the OOD data, we want our model to be as uncertain as possible and this implies high entropy in the predictive distribution. An alternative way to quantify the uncertainty is count-confidence plots, i.e., separate data into bins of the same confidence interval,

dataset	CIFAR10	CIFAR100	SVHN	STL10
size	50000	50000	73257	500
VI	8.51 ± 0.41	8.27 ± 0.40	11.56 ± 0.39	1.75 ± 0.41
DirectUQ	2.18 ± 0.39	2.17 ± 0.43	2.72 ± 0.38	1.16 ± 0.40
SGD	1.97 ± 0.41	1.99 ± 0.43	2.46 ± 0.40	1.12 ± 0.38

Table 1: Running time for training 1 epoch with batch size 512, AlexNet

and then plot the number of data points of each bin as a function of the averaged confidence score. We include the count-confidence plots in the Appendix, as it is not easy to compare multiple methods visually in this manner. Instead, we summarize each count-confidence plot as a single number using the averaged entropy over the entire dataset.

Figure 1(a) and 1(d) show the ECE of each method under data shift. In some cases single-model DirectUQ performs less well than VI. But ensembles of DirectUQ are better than VI, ensembles of SGD and Dropout, and they are even competitive with ensembles of VI. The remaining plots in Figure 1 show the entropy of predictive distribution of OOD data for all methods. Here single-model DirectUQ outperforms SGD and Dropout and ensembles of DirectUQ outperform VI and are even competitive with ensembles of VI. Results for PreResNet20 are similar and they are included in the Appendix (Figure 4).

6.4. In-distribution Log Loss

Figure 2 and Figure 7 (in Appendix) compare VI, DirectUQ and hybrid methods on small datasets. We omit the naive version of DirectUQ as it produces poor results. For regression, duq-mean and duq-mv both perform well and they are better than VI and the hybrid methods in three of four datasets. For classification, duq-l2, i.e., DirectUQ with L2 regularization performs the best among all DirectUQ methods and it is comparable to all VI methods and is better than hybrid methods in three out of four datasets.

Figure 3 and Figure 8 (in Appendix) compare all methods on large datasets. First we observe that using collapsed variational inference in VI does not significantly improve the performance as shown in Tomczak et al. (2021). This is because we use $\eta = 0.1$ that yields better performance while Tomczak et al. (2021) use $\eta = 1$. Second, we observe that duq-mean is the best among all DirectUQ methods and it is worse than VI but better than SGD. SWAG is slightly better in 2 cases but it is significantly worse in other cases. Dropout is not stable across different datasets. Third, we observe that for all methods, ensembles perform better than single models. The ensemble of duq-mean is competitive with VI. Thus, ensembles of DirectUQ can help alleviate the limitation of the expressiveness of DirectUQ. Ensembles of dropout also perform well. Last but not least, we observe that the ensemble of VI performs the best although

optimizing each model in the ensemble is slow. Ensembles of VI have not been well studied in the literature and our experiments highlight their potential strong performance.

Overall, ensembles of DirectUQ are slightly worse but competitive with single model VI and ensembles of Dropout in terms of in-distribution log loss. On the other hand they provide better uncertainty quantification for out of distribution data, which is competitive with ensembles of VI. Among variants, DirectUQ with learn-mean regularizer (duq-mean and ens-duq-mean) provide the best overall performance.

7. Conclusion

In Bayesian neural networks, the distribution of the last layer directly affects the predictive distribution. Motivated by this fact, we proposed direct uncertainty quantification, DirectUQ, that uses a neural network to directly learn the mean and variance of the last layer. We showed that DirectUQ can match the expressive power of VI in linear cases with a strong prior but that in general it provides a less expressive model. On the other hand the simplicity of the model enables fast training and facilitates convergence analysis through Rademacher bounds. In addition, DirectUQ can be derived as a non-standard variational lower bound, which provides an approximation for the last layer. This connection allowed us to derive better regularizations for DirectUQ by using collapsed variational inference over a hierarchical prior. Empirical evaluation highlighted the strong performance of ensembles of VI (when using weak regularization $\eta = 0.1$ instead of 1) albeit at the cost of high run time. Ensembles of DirectUQ are competitive with VI and other methods in terms of in-distribution loss, they outperform VI for out of distribution data, and are even competitive with ensembles of VI. Hence DirectUQ gives a new attractive approach for approximate inference in Bayesian models. The efficiency of DirectUQ also means faster test time predictions which can be important when deploying Bayesian models for real-time applications. In future work it would be interesting to explore the complexity performance tradeoff provided by DirectUQ, and the connections to variational inference in functional space that induces complex priors.

Acknowledgements

This work was partly supported by NSF under grant IIS-1906694. Some of the experiments in this paper were run on the Big Red computing system at Indiana University, supported in part by Lilly Endowment, Inc., through its support for the Indiana University Pervasive Technology Institute.

References

- Blundell, C., Cornebise, J., Kavukcuoglu, K., and Wierstra, D. Weight uncertainty in neural network. In Bach, F. and Blei, D. (eds.), *Proceedings of the 32nd International Conference on Machine Learning*, volume 37 of *Proceedings of Machine Learning Research*, pp. 1613–1622, Lille, France, 07–09 Jul 2015. PMLR. URL <https://proceedings.mlr.press/v37/blundell15.html>.
- Brosse, N., Riquelme, C., Martin, A., Gelly, S., and Moulines, A. On last-layer algorithms for classification: Decoupling representation from uncertainty estimation, 2020. URL <https://arxiv.org/abs/2001.08049>.
- Dua, D. and Graff, C. UCI machine learning repository, 2017. URL <http://archive.ics.uci.edu/ml>.
- Gal, Y. and Ghahramani, Z. Dropout as a bayesian approximation: Representing model uncertainty in deep learning. In *Proceedings of the 33rd International Conference on International Conference on Machine Learning - Volume 48*, ICML’16, pp. 1050–1059. JMLR.org, 2016.
- Golowich, N., Rakhlin, A., and Shamir, O. Size-independent sample complexity of neural networks. In Bubeck, S., Perchet, V., and Rigollet, P. (eds.), *Proceedings of the 31st Conference On Learning Theory*, volume 75 of *Proceedings of Machine Learning Research*, pp. 297–299. PMLR, 06–09 Jul 2018. URL <https://proceedings.mlr.press/v75/golowich18a.html>.
- Graves, A. Practical variational inference for neural networks. In Shawe-Taylor, J., Zemel, R., Bartlett, P., Pereira, F., and Weinberger, K. (eds.), *Advances in Neural Information Processing Systems*, volume 24. Curran Associates, Inc., 2011. URL <https://proceedings.neurips.cc/paper/2011/file/7eb3c8be3d411e8ebfab08eba5f49632-Paper.pdf>.
- Guo, C., Pleiss, G., Sun, Y., and Weinberger, K. Q. On calibration of modern neural networks. In *Proceedings of the 34th International Conference on Machine Learning - Volume 70*, ICML’17, pp. 1321–1330. JMLR.org, 2017.
- He, K., Zhang, X., Ren, S., and Sun, J. Identity mappings in deep residual networks. In Leibe, B., Matas, J., Sebe, N., and Welling, M. (eds.), *Computer Vision – ECCV 2016*, pp. 630–645, Cham, 2016. Springer International Publishing. ISBN 978-3-319-46493-0.
- Higgins, I., Matthey, L., Pal, A., Burgess, C., Glorot, X., Botvinick, M., Mohamed, S., and Lerchner, A. beta-VAE: Learning basic visual concepts with a constrained variational framework. In *International Conference on Learning Representations*, 2017. URL <https://openreview.net/forum?id=Sy2fzU9gl>.
- Izmailov, P., Podoprikin, D., Garipov, T., Vetrov, D. P., and Wilson, A. G. Averaging weights leads to wider optima and better generalization. In Globerson, A. and Silva, R. (eds.), *Proceedings of the Thirty-Fourth Conference on Uncertainty in Artificial Intelligence, UAI 2018, Monterey, California, USA, August 6-10, 2018*, pp. 876–885. AUAI Press, 2018. URL <http://auai.org/uai2018/proceedings/papers/313.pdf>.
- Izmailov, P., Vikram, S., Hoffman, M. D., and Wilson, A. G. G. What are bayesian neural network posteriors really like? In Meila, M. and Zhang, T. (eds.), *Proceedings of the 38th International Conference on Machine Learning*, volume 139 of *Proceedings of Machine Learning Research*, pp. 4629–4640. PMLR, 18–24 Jul 2021. URL <https://proceedings.mlr.press/v139/izmailov21a.html>.
- Kabir, H. M. D., Khosravi, A., Hosen, M. A., and Nahavandi, S. Neural network-based uncertainty quantification: A survey of methodologies and applications. *IEEE Access*, 6:36218–36234, 2018. doi: 10.1109/ACCESS.2018.2836917.
- Kendall, A. and Gal, Y. What uncertainties do we need in bayesian deep learning for computer vision? In Guyon, I., Luxburg, U. V., Bengio, S., Wallach, H., Fergus, R., Vishwanathan, S., and Garnett, R. (eds.), *Advances in Neural Information Processing Systems*, volume 30. Curran Associates, Inc., 2017. URL <https://proceedings.neurips.cc/paper/2017/file/2650d6089a6d640c5e85b2b88265dc2b-Paper.pdf>.
- Khosravi, A., Nahavandi, S., Creighton, D., and Atiya, A. F. Comprehensive review of neural network-based prediction intervals and new advances. *IEEE Transactions on Neural Networks*, 22(9):1341–1356, 2011. doi: 10.1109/TNN.2011.2162110.
- Krizhevsky, A., Sutskever, I., and Hinton, G. E. Imagenet classification with deep convolutional neural networks. In Pereira, F., Burges, C., Bottou, L., and Weinberger, K. (eds.), *Advances in Neural*

- Information Processing Systems*, volume 25. Curran Associates, Inc., 2012. URL <https://proceedings.neurips.cc/paper/2012/file/c399862d3b9d6b76c8436e924a68c45b-Paper.pdf>.
- Lakshminarayanan, B., Pritzel, A., and Blundell, C. Simple and scalable predictive uncertainty estimation using deep ensembles. In Guyon, I., Luxburg, U. V., Bengio, S., Wallach, H., Fergus, R., Vishwanathan, S., and Garnett, R. (eds.), *Advances in Neural Information Processing Systems*, volume 30. Curran Associates, Inc., 2017. URL <https://proceedings.neurips.cc/paper/2017/file/9ef2ed4b7fd2c810847ffa5fa85bce38-Paper.pdf>.
- Li, Y., Hernández-Lobato, J. M., and Turner, R. E. Stochastic expectation propagation. In *Proceedings of the 28th International Conference on Neural Information Processing Systems - Volume 2*, NIPS’15, pp. 2323–2331, Cambridge, MA, USA, 2015. MIT Press.
- Maddox, W. J., Garipov, T., Izmailov, P., Vetrov, D., and Wilson, A. G. *A Simple Baseline for Bayesian Uncertainty in Deep Learning*. Curran Associates Inc., Red Hook, NY, USA, 2019.
- Naeini, M. P., Cooper, G. F., and Hauskrecht, M. Obtaining well calibrated probabilities using bayesian binning. In *Proceedings of the Twenty-Ninth AAAI Conference on Artificial Intelligence*, AAAI’15, pp. 2901–2907. AAAI Press, 2015. ISBN 0262511290.
- Oleksiienko, I., Tran, D. T., and Iosifidis, A. Variational neural networks, 2022. URL <https://arxiv.org/abs/2207.01524>.
- Ovadia, Y., Fertig, E., Ren, J., Nado, Z., Sculley, D., Nowozin, S., Dillon, J. V., Lakshminarayanan, B., and Snoek, J. *Can You Trust Your Model’s Uncertainty? Evaluating Predictive Uncertainty under Dataset Shift*. Curran Associates Inc., Red Hook, NY, USA, 2019.
- Shalev-Shwartz, S. and Ben-David, S. *Understanding Machine Learning - From Theory to Algorithms*. Cambridge University Press, 2014.
- Sun, S., Zhang, G., Shi, J., and Grosse, R. FUNCTIONAL VARIATIONAL BAYESIAN NEURAL NETWORKS. In *International Conference on Learning Representations*, 2019. URL <https://openreview.net/forum?id=rkxacs0qY7>.
- Teh, Y., Hasenclever, L., Lienart, T., Vollmer, S., Webb, S., Lakshminarayanan, B., and Blundell, C. Distributed bayesian learning with stochastic natural gradient expectation propagation and the posterior server. *Journal of Machine Learning Research*, 18, 12 2015.
- Tomczak, M., Swaroop, S., and Turner, R. Efficient low rank gaussian variational inference for neural networks. In Larochelle, H., Ranzato, M., Hadsell, R., Balcan, M., and Lin, H. (eds.), *Advances in Neural Information Processing Systems*, volume 33, pp. 4610–4622. Curran Associates, Inc., 2020. URL <https://proceedings.neurips.cc/paper/2020/file/310cc7ca5a76a446f85c1a0d641ba96d-Paper.pdf>.
- Tomczak, M. B., Swaroop, S., Foong, A. Y. K., and Turner, R. E. Collapsed variational bounds for bayesian neural networks. In Beygelzimer, A., Dauphin, Y., Liang, P., and Vaughan, J. W. (eds.), *Advances in Neural Information Processing Systems*, 2021. URL <https://openreview.net/forum?id=ykN3tbJ0qmX>.
- Tran, B.-H., Rossi, S., Milios, D., and Filippone, M. All You Need is a Good Functional Prior for Bayesian Deep Learning. *Journal of Machine Learning Research*, 23: 1–56, 2022.
- Wenzel, F., Roth, K., Veeling, B. S., Świątkowski, J., Tran, L., Mandt, S., Snoek, J., Salimans, T., Jenatton, R., and Nowozin, S. How good is the bayes posterior in deep neural networks really? In *Proceedings of the 37th International Conference on Machine Learning*, ICML’20. JMLR.org, 2020.
- Wilson, A. G., Izmailov, P., Hoffman, M. D., Gal, Y., Li, Y., Pradier, M. F., Vikram, S., Foong, A., Lotfi, S., and Farquhar, S. Evaluating approximate inference in bayesian deep learning. In Kiela, D., Ciccone, M., and Caputo, B. (eds.), *Proceedings of the NeurIPS 2021 Competitions and Demonstrations Track*, volume 176 of *Proceedings of Machine Learning Research*, pp. 113–124. PMLR, 06–14 Dec 2022. URL <https://proceedings.mlr.press/v176/wilson22a.html>.
- Wu, A., Nowozin, S., Meeds, E., Turner, R. E., Hernandez-Lobato, J. M., and Gaunt, A. L. Deterministic variational inference for robust bayesian neural networks. In *International Conference on Learning Representations*, 2019. URL <https://openreview.net/forum?id=B1l08oAct7>.

A. Proofs

A.1. Proof in Section 3

The next two lemmas extend known bounds for Rademacher complexity through Lipschitz bounds (Shalev-Shwartz & Ben-David, 2014) to functions with multi-dimensional inputs.

Lemma A.1. Consider an L -Lipschitz function $\phi : \mathbb{R} \times \mathbb{R} \rightarrow \mathbb{R}$, i.e. $\phi(a_1, b_1) - \phi(a_2, b_2) \leq L(|a_1 - a_2| + |b_1 - b_2|)$. For $\mathbf{a}, \mathbf{b} \in \mathbb{R}^N$, let $\phi(\mathbf{a}, \mathbf{b})$ denote the vector $(\phi(a_1, b_1), \dots, \phi(a_N, b_N))$. Let $\phi(A \times B)$ denote $\{\phi(\mathbf{a}, \mathbf{b}) : \mathbf{a} \in A, \mathbf{b} \in B\}$, then

$$R(\phi(A \times B)) \leq L(R(A) + R(B)). \quad (17)$$

Proof. We prove the lemma for $L = 1$. If this is not the case, we can define $\phi' = \frac{1}{L}\phi$, and use the fact that $R(\phi(A \times B)) \leq LR(\phi'(A \times B))$. Let $C_i = \{(a_1 + b_1, \dots, a_{i-1} + b_{i-1}, \phi'(a_i, b_i), a_{i+1} + b_{i+1}, \dots, a_N + b_N) : a \in A, b \in B\}$. It suffices to prove that for any set A, B and all i we have $R(C_i) \leq R(A) + R(B)$. Without loss of generality we prove the case for $i = 1$.

$$\begin{aligned} NR(C_1) &= \mathbb{E}_\sigma \left[\sup_{c \in C_1} \sigma_1 \phi(a_1, b_1) + \sum_{i=2}^N \sigma_i (a_i + b_i) \right] \\ &= \frac{1}{2} \mathbb{E}_{\sigma_2, \dots, \sigma_N} \left[\sup_{a \in A, b \in B} \left(\phi(a_1, b_1) + \sum_{i=2}^N \sigma_i (a_i + b_i) \right) + \sup_{a' \in A, b' \in B} \left(-\phi(a'_1, b'_1) + \sum_{i=2}^N \sigma_i (a'_i + b'_i) \right) \right] \\ &= \frac{1}{2} \mathbb{E}_{\sigma_2, \dots, \sigma_N} \left[\sup_{a, a' \in A, b, b' \in B} \left(\phi(a_1, b_1) - \phi(a'_1, b'_1) + \sum_{i=2}^N \sigma_i (a_i + b_i) + \sum_{i=2}^N \sigma_i (a'_i + b'_i) \right) \right] \\ &\leq \frac{1}{2} \mathbb{E}_{\sigma_2, \dots, \sigma_N} \left[\sup_{a, a' \in A, b, b' \in B} \left(|a_1 - a'_1| + |b_1 - b'_1| + \sum_{i=2}^N \sigma_i (a_i + b_i) + \sum_{i=2}^N \sigma_i (a'_i + b'_i) \right) \right] \\ &= \frac{1}{2} \mathbb{E}_{\sigma_2, \dots, \sigma_N} \left[\sup_{a, a' \in A} \left(a_1 - a'_1 + \sum_{i=2}^N \sigma_i a_i + \sum_{i=2}^N \sigma_i a'_i \right) \right] + \frac{1}{2} \mathbb{E}_{\sigma_2, \dots, \sigma_N} \left[\sup_{b, b' \in B} \left(b_1 - b'_1 + \sum_{i=2}^N \sigma_i b_i + \sum_{i=2}^N \sigma_i b'_i \right) \right] \\ &= NR(A) + NR(B). \end{aligned}$$

□

Corollary A.2. Consider an L -Lipschitz function $\phi : \mathbb{R}^d \rightarrow \mathbb{R}$, i.e., for any $x, x' \in \mathbb{R}^d$, $\phi(x) - \phi(x') \leq L\|x - x'\|_1$. Let $\phi(A^d) = \{\phi(a_{1:d,i}) : \mathbf{a}_1, \mathbf{a}_2, \dots, \mathbf{a}_d \in A \subset \mathbb{R}^N\}$, then $R(\phi(A^d)) \leq Ld(R(A))$.

We next verify that Assumption 3.1 holds for classification and (with a modified loss) for regression.

For K -classification, z is K -dimensional and the negative log-likelihood is

$$-\log p(y = k|z) = -\log \frac{\exp(z_k)}{\sum_{i=1}^K \exp(z_i)} = -z_k + \log \sum_{i=1}^K \exp(z_i)$$

which is 1-Lipschitz in z .

For regression, $z = (m, l)$ is 2-dimensional, and the negative log-likelihood is:

$$-\log p(y|z) = \frac{1}{2}(y - m)^2 \exp(-l) + \frac{1}{2}l.$$

Neither the quadratic function nor exponential function is Lipschitz. But we can replace the unbounded quadratic function $(y - m)^2$ with a bounded version $\min\{(y - m)^2, B_m^2\}$, and replace the exponential function $\exp(-l)$ with $\min\{\exp(-l), B_l\}$, where $B > 0$, to guarantee the Lipschitzness. Now the negative log-likelihood is:

$$-\log p(y|z) = \frac{1}{2} \min\{(y - m)^2, B_m^2\} \min\{\exp(-l), B_l\} + \frac{1}{2}l,$$

is $(B_m B_l)$ -Lipschitz in m , $(\frac{1}{2} + \frac{1}{2} B_m^2 B_l)$ -Lipschitz in l .

For Assumption 3.2, we can use $g(l) = \log(1 + \exp(l))$ which is 1-Lipschitz. If $g(l) = \exp(l)$ is the exponential function, we can use a bounded variant that satisfies the requirement $g(l) = \max\{\exp(x), B_g\}$.

A.2. Proof in Section 4

Proof of Theorem 4.2. Consider a neural network with one single hidden layer, denote the weights of the first layer as u , and the weights of the second layer as w . Thus, the k -th output can be computed as:

$$z^{(k)} = \sum_{i=1}^I w_{k,i} \psi \left(\sum_{d=1}^D u_{i,d} x_d \right),$$

where I is the size of the hidden layer, D is the input size and $\psi(a) = \max(0, a)$ is the ReLU activation function. We further simplify the setting by considering the special case where only x_1 is non-zero and $I = 1$. Then the k -th output becomes:

$$z^{(k)} = w_{k,1} \psi(u_{1,1} x_1).$$

Consider a distribution $q(w_{k,i}) = \mathcal{N}(\bar{w}_{k,i}, \sigma_w^2)$, $q(u_{i,d}) = \mathcal{N}(\bar{u}_{i,d}, \sigma_u^2)$. Then if $x_1 \geq 0$,

$$\begin{aligned} \mathbb{E}_{q(w)q(u)} [z^{(k)}] &= \mathbb{E}_{w,u} [w_{k,1} \phi(u_{1,1} x_1)] \\ &= \bar{w}_{k,1} \left(\bar{u}_{1,1} + \frac{\phi(0)}{1 - \Phi(0)} \sigma_u \right) x_1; \end{aligned} \quad (18)$$

if $x_1 < 0$, then

$$\begin{aligned} \mathbb{E}_{q(w)q(u)} [z^{(k)}] &= \mathbb{E}_{w,u} [w_{k,1} \phi(u_{1,1} x_1)] \\ &= \bar{w}_{k,1} \left(\bar{u}_{1,1} - \frac{\phi(0)}{\Phi(0)} \sigma_u \right) x_1, \end{aligned} \quad (19)$$

where ϕ and Φ are the pdf and cdf of standard normal distribution and we directly use the expectation of the truncated normal distribution. Now consider \tilde{w} and \tilde{u} that aim to recover (18) and (19). If $\tilde{u}_{1,1} \geq 0$, it cannot successfully recover (19) because the ReLU activation will have 0 when $x_1 < 0$ so that it cannot recover (19); if $\tilde{u}_{1,1} < 0$, for the same reason it cannot recover (18). \square

B. Derivations of Collapsed Variational Inference

As is shown in (Tomczak et al., 2021), for priors and approximate posteriors from the exponential family, we can derive the closed-form solution for the optimal $q^*(\mu_p, \sigma_p^2)$,

$$\log q^*(\mu_p, \sigma_p^2 | x) \propto \log p(\mu_p, \sigma_p^2) + \mathbb{E}_{q(z|x)} [\log p(z | \mu_p, \sigma_p^2)], \quad (20)$$

for optimizing $q(\mu_p, \sigma_p^2)$ for every single data.

B.1. Learn mean, fix variance

Let $p(z | \mu_p) = \mathcal{N}(z | \mu_p, \gamma I)$, $p(\mu_p) = \mathcal{N}(\mu_p | 0, \alpha I)$. Recall that $q(z | x) = \mathcal{N}(\mu_q(x), \text{diag}(\sigma_q^2(x)))$. Then

$$\begin{aligned} \log q^*(\mu_p | x) &\propto \log p(\mu_p) + \mathbb{E}_{q(z|x)} [\log p(z | \mu_p)] \\ &\propto -\frac{1}{2\alpha} \mu_p^\top \mu_p - \frac{1}{2\gamma} [(\mu_p - \mu_q(x))^\top (\mu_p - \mu_q(x)) + 1^\top \sigma_q^2(x)] \\ &\propto -\frac{\alpha + \gamma}{2\alpha\gamma} \left(\mu_p - \frac{\alpha}{\alpha + \gamma} \mu_q(x) \right)^\top \left(\mu_p - \frac{\alpha}{\alpha + \gamma} \mu_q(x) \right). \end{aligned}$$

Then $q^*(\mu_p) = \mathcal{N}(\frac{\alpha}{\alpha + \gamma} \mu_q(x), \frac{\alpha\gamma}{\alpha + \gamma} I)$. Plugging q^* into the regularizer, the new regularizer becomes

$$\frac{1}{2\gamma} \left[1^\top \sigma_q^2(x) + \frac{\gamma}{\gamma + \alpha} \mu_q(x)^\top \mu_q(x) \right] - \frac{1}{2} 1^\top \log \sigma_q^2(x) + \frac{K}{2} \log(\gamma + \alpha) - \frac{K}{2}.$$

B.2. Learn both mean and variance

Let $p(z|\mu_p, \sigma_p^2) = \mathcal{N}(z|\mu_p, \sigma_p^2)$, $p(\mu_p|\sigma_p^2) = \mathcal{N}(\mu_p|0, \frac{1}{t}\sigma_p^2)$, $p(\sigma_p^2) = \mathcal{IG}(\sigma_p^2|\alpha, \beta)$, where \mathcal{IG} indicates the inverse Gamma distribution. Let $q(\mu_p)$ be a diagonal Gaussian and $q(\sigma_p^2)$ be inverse Gamma. Use $\mu_{p,i}$ and $\sigma_{p,i}$ to denote the i -th entry of μ_p and σ_p respectively, then

$$\begin{aligned} & \log q^*(\mu_{p,i}, \sigma_{p,i}^2) \\ & \propto \log p(\mu_{p,i}, \sigma_{p,i}^2) + \mathbb{E}_{q(z|x)}[\log p(z|\mu_p, \sigma_p^2)] \\ & \propto -(\alpha + \frac{3}{2}) \log \sigma_{p,i}^2 - \frac{2\beta + t\mu_{p,i}^2}{2\sigma_{p,i}^2} - \frac{1}{2} \log \sigma_{p,i}^2 - \frac{1}{2} \frac{(\mu_{p,i} - \mu_{q,i}(x))^2}{\sigma_{p,i}^2} - \frac{1}{2} \frac{\sigma_{q,i}^2(x)}{\sigma_{p,i}^2} \\ & \propto -(\alpha + 2) \log \sigma_{p,i}^2 - \frac{1}{2\sigma_{p,i}^2} \left(2 \left(\beta + \frac{t}{2(t+1)} \mu_{q,i}(x)^2 + \frac{1}{2} \sigma_{q,i}^2(x) \right) + (t+1) \left(\mu_{p,i} - \frac{\mu_{q,i}(x)}{t+1} \right)^2 \right) \end{aligned}$$

follows the normal-inverse-gamma distribution. Thus $q^*(\mu_p|x) = \mathcal{N}(\mu_p|\frac{1}{t+1}\mu_q(x), \frac{1}{t+1}\sigma_p^2)$ and $q^*(\sigma_p^2|x) = \mathcal{IG}(\sigma_p^2|(\alpha + \frac{1}{2})1, \beta + \frac{t}{2(t+1)}\mu_q(x)^2 + \frac{1}{2}\sigma_q^2(x))$. Then the regularizer becomes

$$(\alpha + \frac{1}{2})1^\top \log \left[\beta 1 + \frac{t}{2(1+t)} \mu_q(x)^2 + \frac{1}{2} \sigma_q^2(x) \right] - \frac{1}{2} 1^\top \log \sigma_q^2(x). \quad (21)$$

B.3. Empirical Bayes

Let $p(\sigma_p^2) = \mathcal{IG}(\sigma_p^2|\alpha, \beta)$, $p(z|\sigma_p^2) = \mathcal{N}(z|0, \sigma_p^2 I)$, and let $q(\sigma_p^2)$ be a delta distribution. Then

$$\begin{aligned} & \text{KL}(q(z|x)||p(z|\sigma_p^2)) - \log p(\sigma_p^2) \\ & = \frac{1}{2} \left[K \log \sigma_p^2 - 1^\top \log \sigma_q^2(x) - K + \frac{1^\top \sigma_q^2(x)}{\sigma_p^2} + \frac{\mu_q(x)^\top \mu_q(x)}{\sigma_p^2} \right] + (\alpha + 1) \log \sigma_p^2 + \frac{\beta}{\sigma_p^2}. \end{aligned}$$

By taking the derivatives of the above equation with respect to σ_p^2 and solving, we obtain the optimal $\sigma_p^2 = \frac{\mu_q(x)^\top \mu_q(x) + 1^\top \sigma_q^2(x) + 2\beta}{K + 2\alpha + 2}$. If we plug this back into the KL term, we get the eq (16). However, if we include the negative log-prior term $(\alpha + 1) \log \frac{\mu_q(x)^\top \mu_q(x) + 1^\top \sigma_q^2(x) + 2\beta}{K + 2\alpha + 2} + \beta \frac{K + 2\alpha + 2}{\mu_q(x)^\top \mu_q(x) + 1^\top \sigma_q^2(x) + 2\beta}$, adding them up we will have

$$\frac{1}{2} (K + 2\alpha + 2) \log \frac{\mu_q(x)^\top \mu_q(x) + 1^\top \sigma_q^2(x) + 2\beta}{K + 2\alpha + 2} - 1^\top \log \sigma_q^2(x) + \text{const},$$

which highly reduces the complexity of the regularizer. This performs less well in practice and therefore we follow (Wu et al., 2019) and use eq (16).

C. Optimizing the Variational Distribution for All Data

In the previous section we show the derivation of collapsed variational inference where $q^*(\mu_p, \sigma_p^2)$ is optimized for every data point x . In this section we show how to optimize $q(\mu_p, \sigma_p^2)$ for all data and obtain different regularizers to the ones mentioned in the above section. These perform less well in practice but we include them here for completeness. The closed-form solution for $q^*(\mu_p, \sigma_p^2)$ for all data is

$$\log q^*(\mu_p, \sigma_p^2) \propto \frac{1}{N} \sum_{(x,y) \in \mathcal{D}} \left\{ \log p(\mu_p, \sigma_p^2) + \mathbb{E}_{q(z|x)}[\log p(z|\mu_p, \sigma_p^2)] \right\}. \quad (22)$$

C.1. Learn mean, fix variance, optimize for all data

Let $p(z|\mu_p) = \mathcal{N}(z|\mu_p, \gamma)$, $p(\mu_p) = \mathcal{N}(\mu_p|0, \alpha)$. Given a dataset $\mathcal{D} = \{(x, y)\}$, we can get one optimal $q^*(\mu_p)$ for all data. According to eq (22),

$$\begin{aligned} \log q^*(\mu_p) &\propto \frac{1}{N} \sum_{(x,y) \in \mathcal{D}} \left\{ \log p(\mu_p) + \mathbb{E}_{q(z|x)}[\log p(z|\mu_p)] \right\} \\ &\propto -\frac{1}{2\alpha} \mu_p^\top \mu_p - \frac{1}{2\gamma N} \sum_{(x,y) \in \mathcal{D}} ((\mu_p - \mu_q(x))^\top (\mu_p - \mu_q(x)) + 1^\top \sigma_q^2(x)) \\ &\propto -\frac{\alpha + \gamma}{2\alpha\gamma} \left(\mu_p - \frac{1}{N} \sum_{(x,y) \in \mathcal{D}} \mu_q(x) \right)^\top \left(\mu_p - \frac{1}{N} \sum_{(x,y) \in \mathcal{D}} \mu_q(x) \right). \end{aligned}$$

Then the optimal $q^*(\mu_p) = \mathcal{N}(\frac{\alpha}{\alpha+\gamma} \frac{1}{N} \sum_x \mu_q(x), \frac{\alpha\gamma}{\alpha+\gamma} I)$. Let $\bar{\mu}_q = \frac{1}{N} \sum_x \mu_q(x)$. The regularizer now is:

$$\begin{aligned} &\sum_{(x,y)} \left\{ \mathbb{E}_{q(\mu_p)} [\text{KL}(q(z|x)||p(z|\mu_p, \gamma))] + \text{KL}(q(\mu_p)||p(\mu_p)) \right\} \\ &= \sum_{(x,y)} \left\{ \mathbb{E}_{q(\mu_p)} \left[K \log \gamma - 1^\top \log \sigma_q^2(x) - K + \frac{1}{\gamma} 1^\top \sigma_q^2(x) - \frac{1}{\gamma} (\mu_q(x) - \mu_p)^\top (\mu_q(x) - \mu_p) \right] \right\} \\ &\quad + \frac{N}{2} \left[K \log \frac{\alpha + \gamma}{\gamma} - K + K \frac{\gamma}{\gamma + \alpha} + \frac{\alpha^2}{(\alpha + \gamma)^2} \bar{\mu}_q^\top \bar{\mu}_q \right] \\ &= \sum_{(x,y)} \left\{ \frac{1}{2\gamma} (1^\top \sigma_q^2(x) + \mu_q(x)^\top \mu_q(x)) - \frac{1}{2} 1^\top \log \sigma_q^2(x) \right\} - \frac{N}{2} \left(\frac{1}{\gamma} - \frac{1}{\alpha + \gamma} \right) \bar{\mu}_q^\top \bar{\mu}_q + \frac{NK}{2} \log(\alpha + \gamma) - \frac{NK}{2}. \end{aligned} \tag{23}$$

We refer to this method as “duq-mean_all”.

C.2. Learn both mean and variance, optimize mean for single data, and variance for all data

Let $p(z|\mu_p, \sigma_p^2) = \mathcal{N}(z|\mu_p, \sigma_p^2)$, $p(\mu_p|\sigma_p^2) = \mathcal{N}(\mu_p|0, \frac{1}{t} \sigma_p^2)$, $p(\frac{1}{\sigma_p^2}) = \mathcal{IG}(\frac{1}{\sigma_p^2}|\alpha, \beta)$. Consider that

$$\log p(\mu_{p,i}, \sigma_{p,i}^2) + \mathbb{E}_{q(z|x)}[\log p(z|\mu_{p,i}, \sigma_{p,i}^2)] \tag{24}$$

$$= \log p(\mu_{p,i}|\sigma_{p,i}^2) + \log p(\sigma_{p,i}^2) + \mathbb{E}_{q(z|x)}[\log p(z|\mu_{p,i}, \sigma_{p,i}^2)] \tag{25}$$

$$\propto -\frac{t}{2} \frac{\mu_{p,i}^2}{\sigma_{p,i}^2} - \frac{1}{2} \log \sigma_{p,i}^2 - (\alpha + 1) \log \sigma_{p,i}^2 - \frac{\beta}{\sigma_{p,i}^2} - \frac{1}{2} \log \sigma_{p,i}^2 - \frac{1}{2\sigma_{p,i}^2} ((\mu_{p,i} - \mu_{q,i}(x))^2 + \sigma_{q,i}^2(x)) \tag{26}$$

$$= -\frac{t}{2} \frac{\mu_{p,i}^2}{\sigma_{p,i}^2} - \log \sigma_{p,i}^2 - (\alpha + 1) \log \sigma_{p,i}^2 - \frac{\beta}{\sigma_{p,i}^2} - \frac{1}{2\sigma_{p,i}^2} ((\mu_{p,i} - \mu_{q,i}(x))^2 + \sigma_{q,i}^2(x)), \tag{27}$$

$$= -\frac{t+1}{2\sigma_{p,i}^2} \left(\mu_{p,i} - \frac{1}{t+1} \mu_{q,i}(x) \right)^2 - \frac{t\mu_{q,i}^2(x)}{2(t+1)\sigma_{p,i}^2} - (\alpha + 2) \log \sigma_{p,i}^2 - \frac{\beta}{\sigma_{p,i}^2} - \frac{\sigma_{q,i}^2(x)}{2\sigma_{p,i}^2} \tag{28}$$

Then by extracting the μ_p part from eq (28), we have

$$\log q^*(\mu_{p,i}|\sigma_{p,i}^2, x) \propto -\frac{t+1}{2\sigma_{p,i}^2} \left(\mu_{p,i} - \frac{1}{t+1} \mu_{q,i}(x) \right)^2,$$

and thus $q^*(\mu_p|x, \sigma_p^2) = \mathcal{N}(\mu_p|\frac{1}{t+1}\mu_q(x), \frac{1}{t+1}\sigma_p^2)$. Then we try to marginalize out μ_p to compute $q^*(\sigma_p^2)$.

$$\begin{aligned}
 \log q^*(\sigma_{p,i}^2) &\propto \frac{1}{N} \sum_{(x,y) \in \mathcal{D}} \log \int \exp(\log p(\mu_{p,i}, \sigma_{p,i}^2) + \mathbb{E}_{q(z|x)}[\log p(z|\mu_{p,i}, \sigma_{p,i}^2)]) d\mu_{p,i} \\
 &\propto \frac{1}{N} \sum_{x,y \in \mathcal{D}} \left\{ \frac{1}{2} \log \int \exp \left(-\frac{t+1}{2\sigma_{p,i}^2} \left(\mu_{p,i} - \frac{1}{t+1} \mu_{q,i}(x) \right)^2 \right) d\mu_{p,i} \right. \\
 &\quad \left. - \frac{t\mu_{q,i}^2(x)}{2(t+1)\sigma_{p,i}^2} - (\alpha+2) \log \sigma_{p,i}^2 - \frac{\beta}{\sigma_{p,i}^2} - \frac{\sigma_{q,i}^2(x)}{2\sigma_{p,i}^2} \right\} \\
 &= -(\alpha+2) \log \sigma_{p,i}^2 - \frac{\beta}{\sigma_{p,i}^2} + \frac{1}{N} \sum_{(x,y) \in \mathcal{D}} \left(\frac{1}{2} \log \frac{2\pi\sigma_{p,i}^2}{t+1} - \frac{\sigma_{q,i}^2(x)}{2\sigma_{p,i}^2} - \frac{t\mu_{q,i}^2(x)}{2(t+1)\sigma_{p,i}^2} \right) \\
 &= -(\alpha + \frac{3}{2}) \log \sigma_{p,i}^2 - \frac{\beta + \frac{t}{2(t+1)} \frac{1}{N} \sum \mu_{q,i}^2(x) + \frac{1}{2N} \sum \sigma_{q,i}^2(x)}{\sigma_{p,i}^2},
 \end{aligned}$$

and $q^*(\sigma_p^2) = \mathcal{IG}(\sigma_p^2 | (\alpha + \frac{1}{2})1, \beta + \frac{t}{2(t+1)} \frac{1}{N} \sum_x \mu_q(x)^2 + \frac{1}{2} \frac{1}{N} \sum_x \sigma_q^2(x))$. Let $\tilde{\mu}_q = \sqrt{\frac{1}{N} \sum_x \mu_q(x)^2}$ and $\tilde{\sigma}_q = \sqrt{\frac{1}{N} \sum_x \sigma_q(x)^2}$, then the regularizer becomes:

$$(\alpha + \frac{1}{2})N1^\top \log \left[\beta 1 + \frac{t}{2(1+t)} \tilde{\mu}_q^2 + \frac{1}{2} \tilde{\sigma}_q^2 \right] - \sum_{(x,y)} \frac{1}{2} 1^\top \log \sigma_q^2(x) \quad (29)$$

$$+ KN \log \frac{\Gamma(\alpha)}{\Gamma(\alpha + \frac{1}{2})} - NK\alpha \log \beta + \frac{NK}{2} \log \frac{t+1}{t} - \frac{NK}{2}. \quad (30)$$

We refer to this method as “duq-mv_all”.

C.3. Empirical Bayes for all data

If we optimize σ_p^2 for all data, then we have

$$\begin{aligned}
 &\sum_{(x,y) \in \mathcal{D}} \left\{ \text{KL}(q(z|x)||p(z|\sigma_p^2)) - \log p(\sigma_p^2) \right\} \\
 &= \sum_{(x,y) \in \mathcal{D}} \left\{ \frac{1}{2} \left[K \log \sigma_p^2 - 1^\top \log \sigma_q^2(x) - K + \frac{1^\top \sigma_q^2(x)}{\sigma_p^2} + \frac{\mu_q(x)^\top \mu_q(x)}{\sigma_p^2} \right] + (\alpha+1) \log \sigma_p^2 + \frac{\beta}{\sigma_p^2} \right\}
 \end{aligned}$$

and the optimal variance being $\frac{\tilde{\mu}_q^\top \tilde{\mu}_q + 1^\top \tilde{\sigma}_q^2 + 2\beta}{K+2\alpha+2}$ where $\tilde{\mu}_q = \sqrt{\frac{1}{N} \sum_x \mu_q(x)^2}$ and $\tilde{\sigma}_q = \sqrt{\frac{1}{N} \sum_x \sigma_q(x)^2}$. The objective is:

$$\begin{aligned}
 &\frac{NK}{2} \log \frac{2\beta + \tilde{\mu}_q^2 + \tilde{\sigma}_q^2}{K+2\alpha+2} - \frac{1}{2} \sum_x 1^\top \log \sigma_q(x)^2 - \frac{NK}{2} \\
 &+ \frac{1}{2} \frac{K+2\alpha+2}{2\beta + \tilde{\mu}_q^2 + \tilde{\sigma}_q^2} \sum_x (\mu_q(x)^\top \mu_q(x) + 1^\top \sigma_q^2(x)).
 \end{aligned}$$

This method is called “duq-eb_all”.

D. Experimental Details

In this section we elaborate the experimental details, including the choice of hyperparameters, learning rates and the number of training epochs. Since all experiments use the same sets of hyperparameters for collapsed variational inference, we introduce these here. For collapsed variational inference, we pick $\gamma = 0.3$, $\alpha_{reg} = \frac{\gamma}{\alpha+\gamma} = 0.05$ for learn-mean regularizer

(vi-mean, duq-mean, duq-mean-all) and $\alpha = 0.5, \beta = 0.01, \delta = \frac{t}{1+t} = 0.1$ for learn-mean-variance regularizer (vi-mv, duq-mv, duq-mv_all), which exactly follows (Tomczak et al., 2021). We pick $\alpha = 4.4798$ and $\beta = 10$ for empirical Bayes (vi-eb, duq-eb, duq-eb_all). The choice of α in empirical Bayes follows (Wu et al., 2019) but the choice of β is unclear in (Wu et al., 2019) so we just perform a simple search from $\{1, 10, 100\}$ and set $\beta = 10$ that yields the best result.

Next we list the choices of the variance for naive methods. The choice of prior variance significantly affects the performance. For UCI classification and regression tasks, we set the prior variance to be 0.1 for both vi-naive and duq-naive. For image datasets with complex neural networks, the total prior variance of VI grows with the number of parameters so we have to pick a small variance and we use 0.05 following the setting in (Wilson et al., 2022). Since DirectUQ samples in the output space which is small, using 0.05 regularizes too strongly and we therefore set a larger value of 1 for the variance. For all VI and DirectUQ methods, we use the Adam optimizer with learning rate 0.001, except that we choose learning rate 0.0005 for boston and concrete which are hard to optimize.

We next list the details for running the hybrid methods, including SGD, SWA and SWAG. The hybrid methods are not very stable so we have to tune learning rates carefully for each dataset. We choose the momentum to be 0.9 for all cases and list all other information in Table 2. Notice that it is hard to train the hybrid methods on SVHN using AlexNet, so we initialize with a pre-trained model that is trained with a larger learning rate 0.1 to find a region with lower training loss, and then continue to optimize with the parameters listed in Table 2. Our code will be available when the paper is published.

	lr	wd	swag_lr	swag_start	epochs
UCI Classification	0.001	0.001	0.001	1001	2000
boston	0.0005	0.001	0.0005	1001	5000
concrete	0.0005	0.1	0.0005	1001	5000
yacht	0.001	0.001	0.001	1001	5000
power	0.001	0.1	0.001	1001	5000
CIFAR10 / CIFAR100	0.05	0.0001	0.01	161	500
SVHN*	0.001	0.0001	0.005	161	500
STL10	0.05	0.001	0.01	161	500

Table 2: The parameters for running the hybrid algorithms. “lr” means the learning rate, “wd” means weight decay, “swag_lr” means the learning rate after we start collecting models in SWA and SWAG algorithms, “swag_start” means the epochs when we start to collect models, “epochs” is the number of training epochs.

E. Additional Experimental Results

In this section we list the results that are not in main paper due to space limit. We also include the comparisons of all methods we mentioned, including those in Section C.

E.1. Uncertainty Quantification for Shifted and Out-of-distribution Data

Figure 4 shows the same uncertainty quantification measures as Figure 1 but on PreResNet20.

Figure 5 and 6 are the count-confidence curves. “A→B” in the subcaptions means we train the model on dataset A and predict on a completely out-of-distribution dataset B. For each example in B, we obtain the class probabilities and choose the maximum probability to be the confidence score and the corresponding class label to be the prediction. Then we separate interval $[0, 1]$ into 10 buckets of the same length and put all examples into these buckets according to their confidence scores. For each bucket, we compute the average confidence score and the proportion of examples that fall into this bucket and then plot the count-confidence curves. Since the dataset B is a complete out-of-distribution dataset for A, we want the confidence score to be as small as possible. So an algorithm with good uncertainty quantification will put more data in the low-confidence region and less data in the high confidence region. In this sense, we observe that the ensembles perform better than the single models, single-model DirectUQ performs better than SGD and worse than VI and the ensemble of DUQ performs comparably to the ensemble of VI. Notice that the ensemble of DirectUQ costs much less time than the ensemble of VI, which confirms our conclusion in the main paper that the ensemble of DirectUQ provides the best tradeoff between run time and the uncertainty quantification.

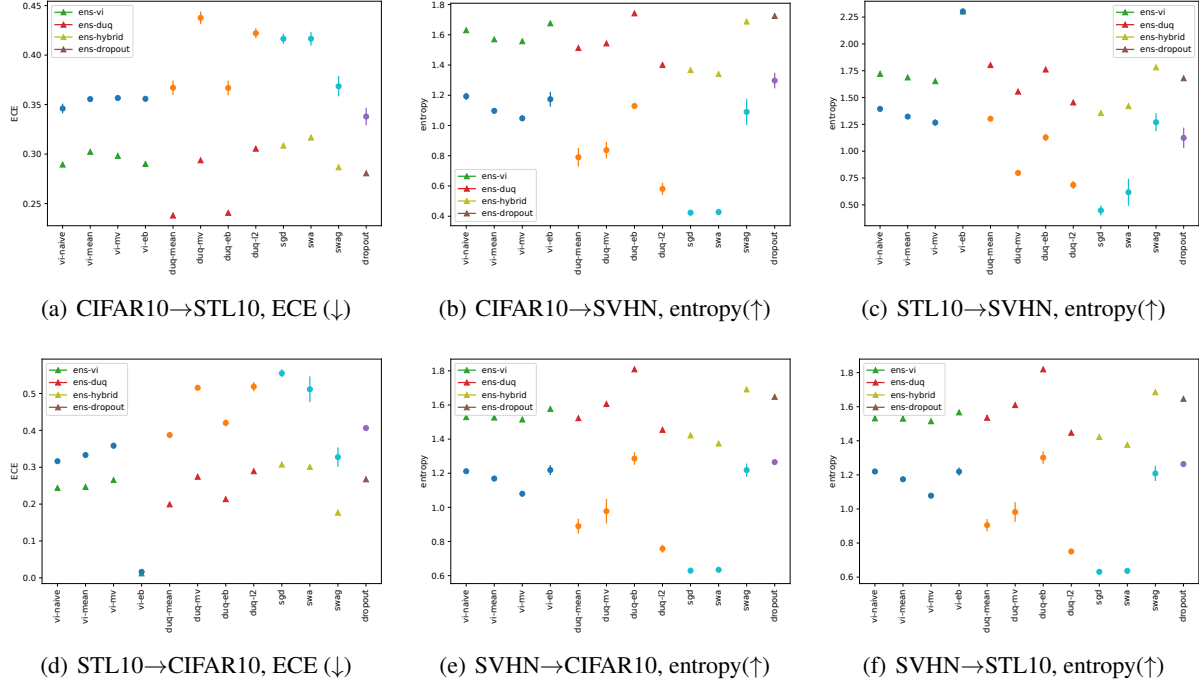


Figure 4: Uncertainty Quantification on PreResNet20

E.2. In-distribution Log Loss

Figures 9, 10, 11 and 12 show a full version of comparison between VI, DirectUQ and the hybrid methods, including duq-naive, duq-mean_all, duq-mv_all and duq-eb_all. As we can see, duq-naive performs the worst and duq-mean_all, duq-mv_all and duq-eb_all perform worse than their counterparts, duq-mean, duq-mv and duq-eb.

E.3. In-distribution Accuracy

For completeness, we add the comparison in terms of the accuracy. Results are shown in Figures 13, 14, 15 and 16. The comparisons of accuracy between VI, DUQ and the hybrid methods are consistent with those of log loss.

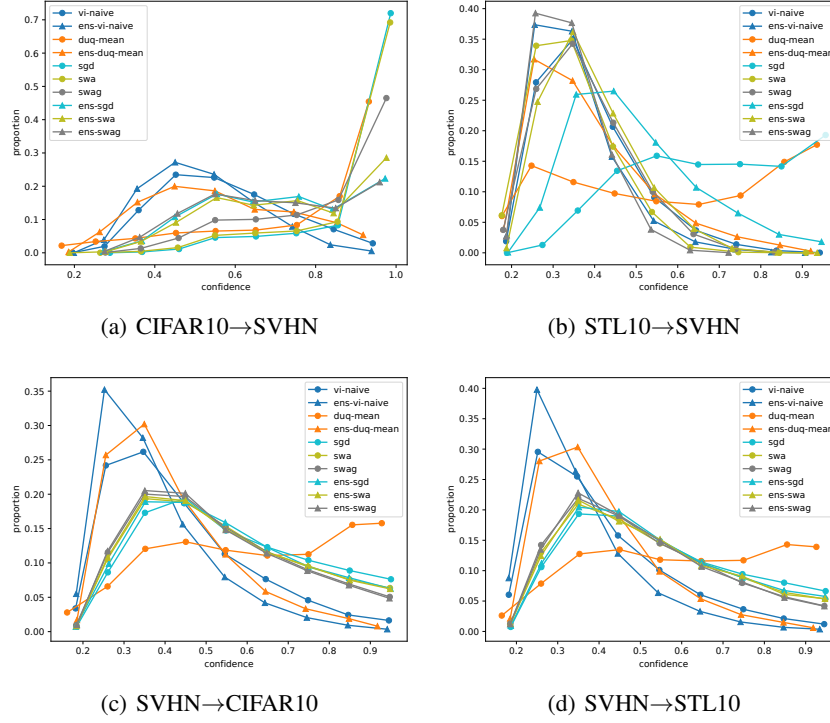


Figure 5: Count-confidence curves, AlexNet. X-axis is the confidence score, y-axis is the proportion of data that have the same range of confidence scores.

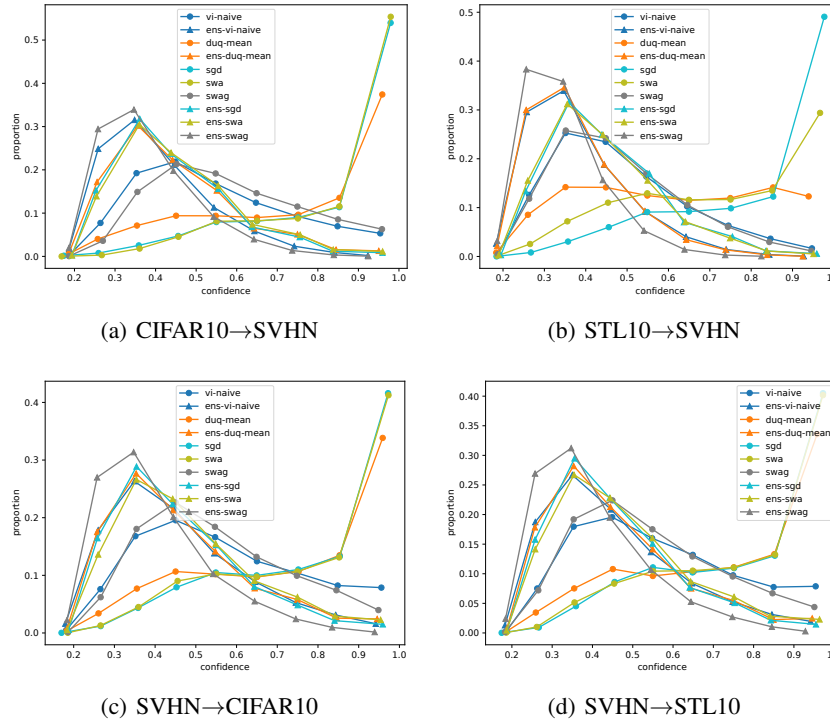


Figure 6: Count-confidence curves, PreResNet20

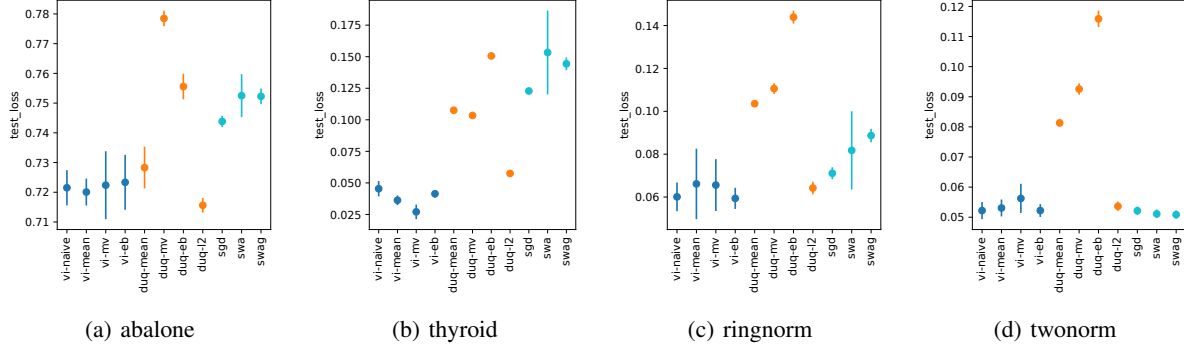


Figure 7: Test log loss on UCI classification datasets. Each dot with the error bar shows the mean and standard deviation of 5 independent runs. The standard deviations for some methods are very small.

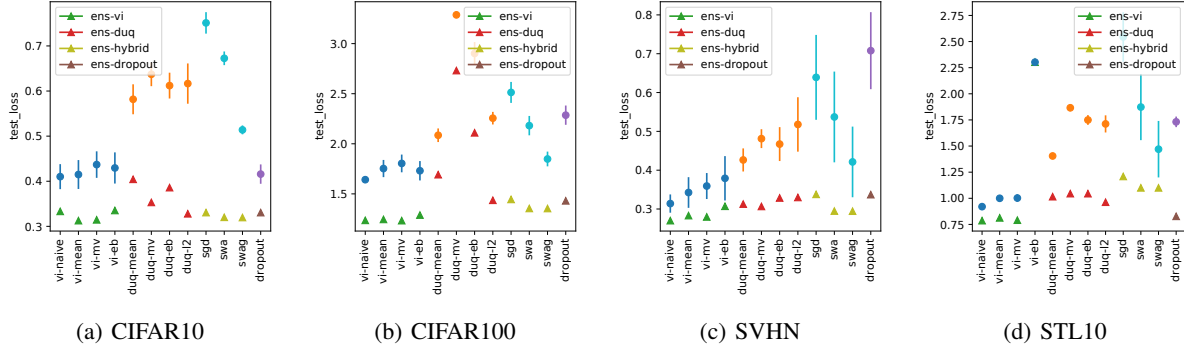


Figure 8: Test log loss of four image datasets on PreResNet20.

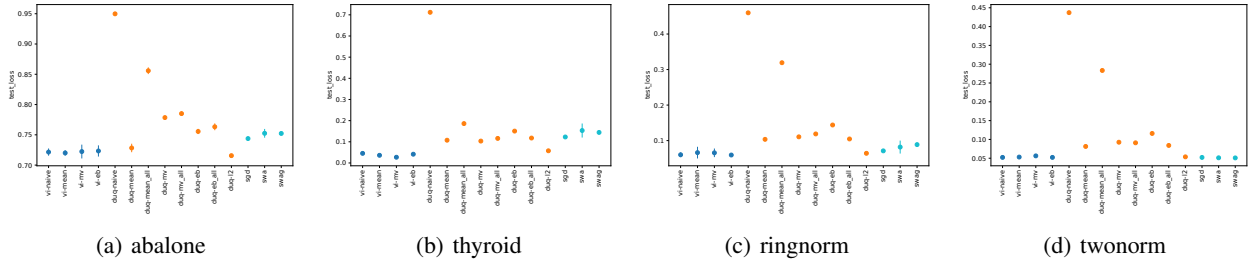


Figure 9: Test log loss on UCI classification datasets.

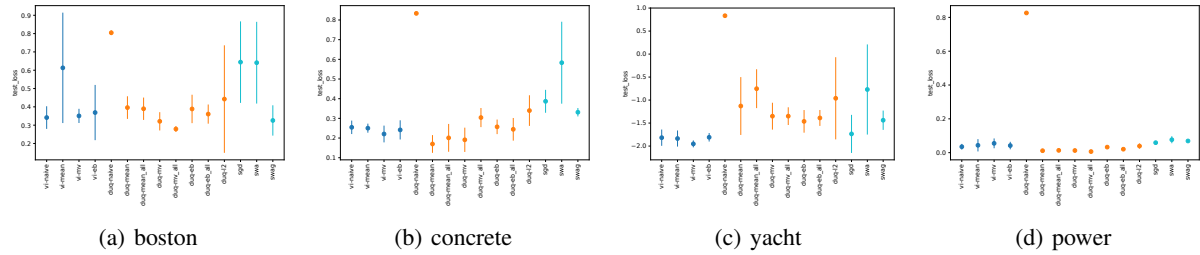


Figure 10: Test log loss on UCI regression datasets.

Direct Uncertainty Quantification

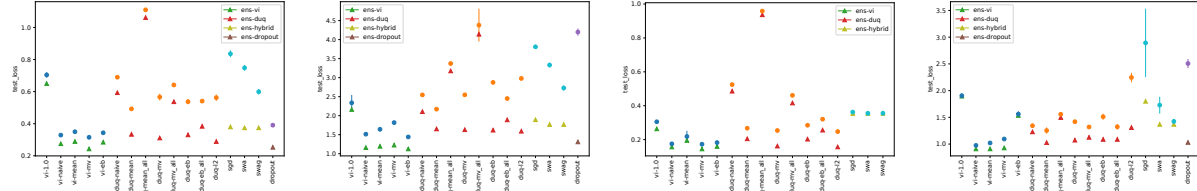


Figure 11: Test log loss of four image datasets on AlexNet.

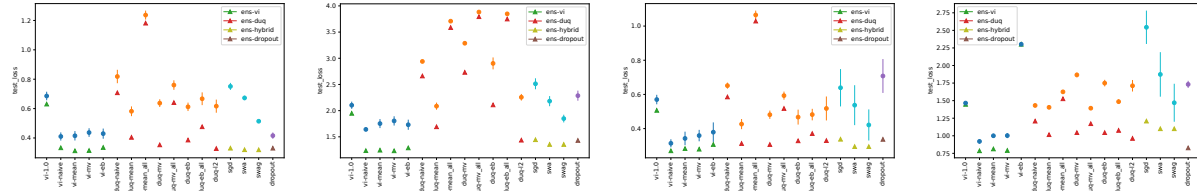


Figure 12: Test log loss of four image datasets on PreResNet20.

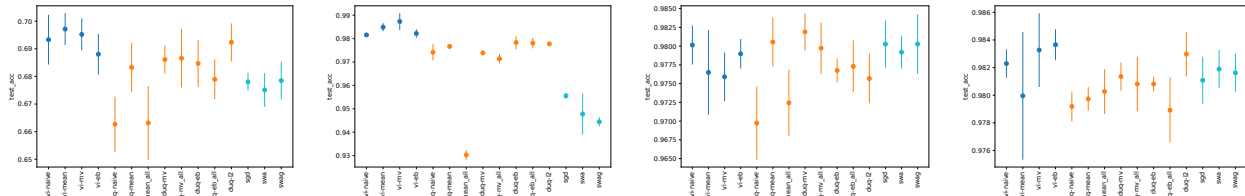


Figure 13: Test accuracy on UCI classification datasets.

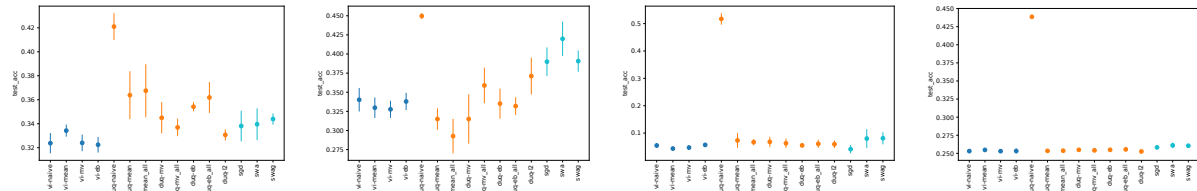


Figure 14: Test RMSE (↓) on UCI regression datasets.

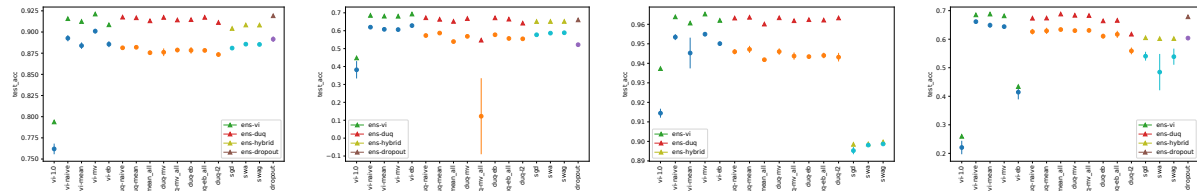


Figure 15: Test accuracy of four image datasets on AlexNet.

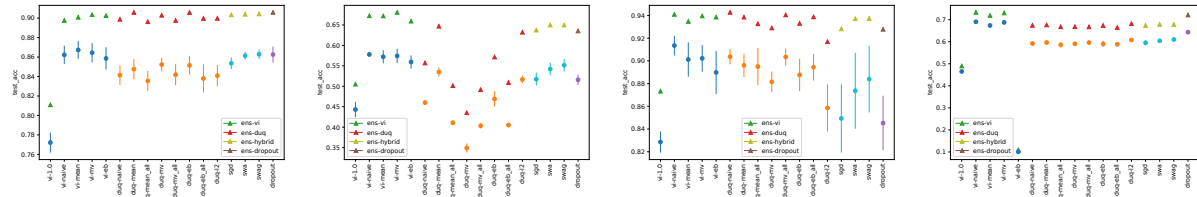


Figure 16: Test accuracy of four image datasets on PreResNet20.